DOI 10.5162/sensoren2016/4.4.1

Permittivity Measurement with a Radio Communication System

Iurii Motroniuk, Stephan Hummel, Alice Fischerauer, Gerhard Fischerauer
Chair of Measurement and Control Systems, Universität Bayreuth, 95440 Bayreuth, Germany
mrt@uni-bayreuth.de

Abstract

We have recently proposed a measurement approach based on the fact that the stochastic parameters of a microwave communication system depend on the properties of the materials in the microwave propagation path. This has been demonstrated to be a possible means of estimating the state of catalysts inside metallic housings in situ and from the outside of the catalyst. In this contribution, we show that the method may be applied to the quantitative determination of the dielectric permittivity of samples inside a microwave cavity resonator. Measurements were performed on samples made of polytetrafluoroethylene (PTFE), polyethylene (PE), polycarbonate (PC), and polyoxymethylene (POM).

Keywords: permittivity measurement, NDE, microwave-based, communication channel, stochastic parameters.

Introduction

The cavity perturbation technique is a well-established method for the non-destructive determination of material properties. In this technique, the properties of a sample under test are extracted from the changes in the resonance characteristics of an empty microwave cavity resonator when this resonator is loaded with the sample. Usually, one measures the scattering parameters of the resonator with a vector network analyzer, or VNA [1, 2].

While VNAs are readily available in the laboratory, the approach does not lend itself to field applications with a certain size or cost sensitivity. The few attempts at reducing the size of the equipment have not been published in enough detail to allow independent tests, let alone that they have led to commercially available products [3].

We have demonstrated previously that it may be possible to replace the VNA with standard inexpensive radio communication hardware. More specifically, we have shown that the received signal in such a communication system responds to the catalyst state in an exhaust gas aftertreatment system if the catalyst-loaded cavity is used as transmission channel [4, 5]. The results led us to believe that the load level of the catalyst (a deterministic parameter) can be estimated from stochastic communication system parameters such as the bit error ratio (BER), the packet error ratio (PER), the ratio of the energy per bit to the noise power spectral density E_b/N_0, the data receive rate (Rx data rate) [4] or the received waveform characteristics in an ultra-wideband (UWB) system [5, 6]. This use of random variables for the estimation of deterministic variables may be called a stochastic measurement approach. We have now applied this stochastic approach to the problem of non-destructive material testing.

Wireless Approach

Let us consider the interior of the metallic housing as a communication channel between two terminals of a UWB radio communication system, as it was proposed for the catalytic converters in [4, 5]. The communication system parameters depend on the characteristics of this channel. The signal transmitted through the channel suffers from such effects as attenuation, fading, multipath propagation, scattering, etc. As these effects will be influenced ba a material sample placed in the channel, it should be possible to estimate the material properties – we are interested in the dielectric permittivity – from the measured or estimated channel characteristcis.

The effect of the sample on the signal is similar to the effect of buildings, trees, autos, rain, humidity, etc. in common radio communication

links: the channel characteristics influence the signal waveform received. Here, the closed-space propagation through the sample-loaded cavity resonator medium affects the received signal waveform.

Channel estimation is a common task in radio communication systems. Note, however, that the transmitter and receiver in such a system are located in the far field of each other whereas, in the present context, they are located in the near field. This, together with the resonance phenomena in the sample-filled microwave cavity, introduces new propagation-path effects compared to wireless transmission links.

The estimation of the sample properties via communication system parameters means that this measurement task can be performed by existing hardware (wireless communication modules) and software (signal processing techniques for radio communication systems). This promises considerable architectural simplicity. However, a prerequisite for this is that the relationship between the system parameters and the material parameters are either known or are established by calibration measurements.

To investigate the principle further, we used the UWB system Time Domain PulsON P410 for signal generation, transmission, and reception. The corresponding nodes generate UWB pulses with a spectrum ranging from 3.1 to 5.3 GHz [7]. The spectrum was characterized with a signal source analyzer Rohde&Schwarz FSUP26 (Fig. 1; during the measurement the UWB module was directly connected to the signal source analyzer with a 50-Ω coaxial cable, and a transmit power of P_{Tx} = −14.6 dBm was used).

Fig. 2 shows the time-domain signal picked up by the UWB receiver module, when the transmission occurs via an empty microwave cavity resonator (P_{Tx} = −64.62 dBm). The vertical scale represents A-D (analog-to-digital) counts proportional to volts as output by the analog-to-digital converter (ADC) in the receiver module.

The envelopes $e(t)$ of time-domain signals such as the one shown in Fig. 2 were computed as the magnitude of the analytic signal constructed from the original signal $u(t)$ by adding to it its Hilbert transform [8]:

$$e(t) = |\, u(t) + \mathrm{j}\hat{u}(t) \,| \text{ with } \hat{u}(t) = \frac{1}{\pi} \int_{-\infty}^{\infty} \frac{u(\tau)}{t-\tau} \mathrm{d}\tau \,. \quad (1)$$

The result for the signal of Fig. 2 is shown in Fig. 3.

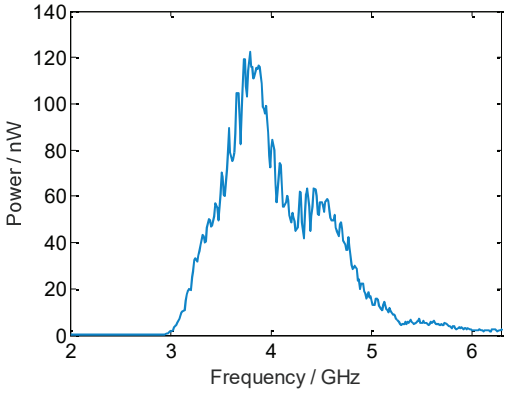

Fig. 1: Measured frequency spectrum of the UWB modules used.

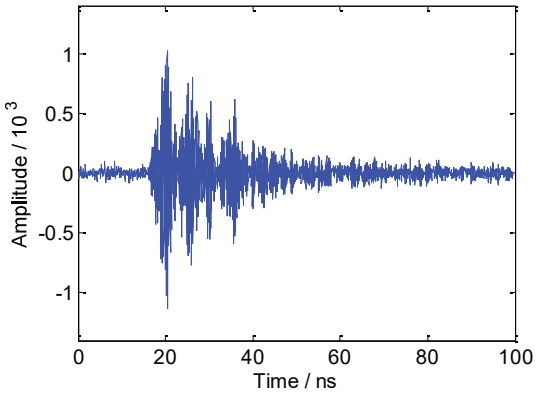

Fig.2: Time-domain receive signal of a UWB pulse transmitted via an empty metallic cavity resonator.

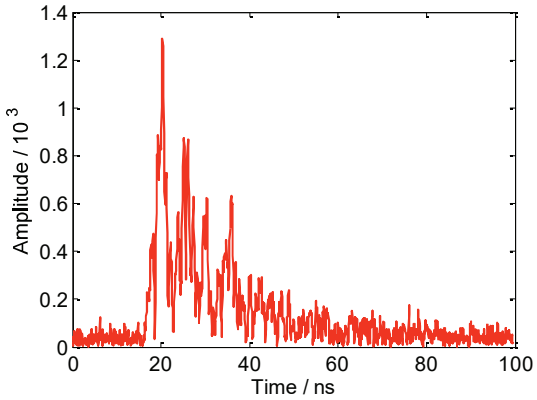

Fig. 3: Envelope of the UWB signal shown in Fig. 2.

Experimental Setup

Our measurement system consists of a circular cylindrical microwave cavity resonator which is partially filled with a disc-shaped sample of the material under test (the discs being held in place by thin rubber rings; Fig. 4). Two short-stub feeds are used as couplers and are connected with the system environment by coaxial cables. This environment consists of identical UWB transceiver modules as source and sink, respectively.

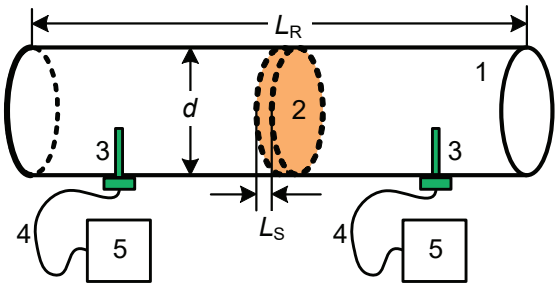

Fig. 4: Schematic drawing of the test system. 1: Cavity resonator. 2: Sample of material under test. 3: Short-stub couplers. 4: 50-Ω coaxial cables. 5: Communication transceiver modules.

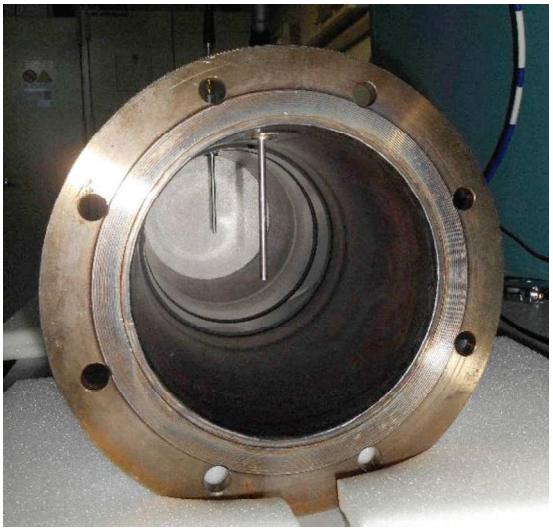

Fig. 5: Inside view of the cavity resonator with stub couplers and rubber rings.

Tab. 1: Listing of materials investigated.

Name	Relative permittivity ε_r [9, 10]
Polytetrafluoroethylene (PTFE)	2.05
Polyethylene (PE)	2.3 … 2.4
Polycarbonate (PC	3.0
Polyoxymethylene (POM)	3.8
Acrylonitrile-butadiene-styrene (ABS)	2.0 … 3.5

It was checked by measurements that the two rubber rings used to hold the material sample in place had a negligible effect on the resonant behavior of the cavity. Fig. 5 shows the interior of the cavity resonator.

We have tested discs made of various materials (all 124.5 mm in diameter and 10 mm thick). Table 1 lists the nominal relative permittivities (dielectric constants) of these materials according to [9, 10].

Tab. 2: Measured relative permittivities.

Material	Measured ε_r @ 1 MHz
PTFE	2.11
PE	2.43
PC	3.06
POM	3.57

We have also characterized the samples by an LCR meter Agilent E4980A in a parallel-plate capacitor setup. By comparing the measured capacitances of the empty capacitor with those of the sample-loaded capacitor (corrected for the capacitances of the connecting cables), it was possible to determine the relative permittivity of the sample materials (Table 2).

Of course, the permittivities listed in Tables 1 and 2 are low-frequency values whereas the cavity perturbation method yields high-frequency values. For materials with low-frequency permittivities below about 4, the 1-GHz value may be lower by 0.2 to 0.4 [11].

Results

Fig. 6 shows the measured packet error ratio PER of the UWB-link measurement system as a function of the transmit power P_{Tx} and of the material sample (hence, as a function of ε_r). It is obvious that PER should depend on P_{Tx} as more power means better signal-to-noise ratio, which in turn means fewer bit and packet errors.

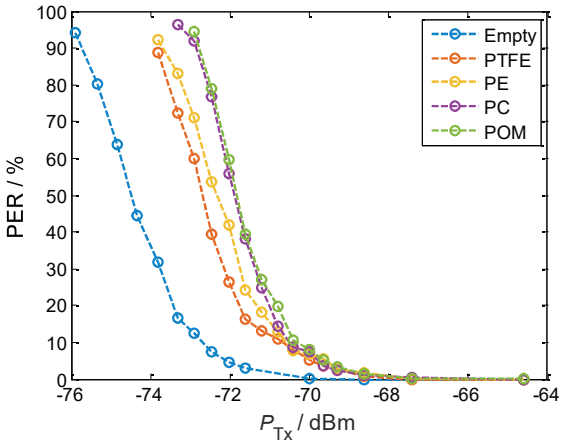

Fig. 6: Measured PER in a UWB system communicating via a disc-loaded cavity resonator as a function of the transmitter power and the sample material. In all instances, the time window to determine PER was 300 s.

The dependence on the material in the propagation path is explained as follows: the standing-wave pattern in the cavity depends on the relative permittivity ε_r of the disc-shaped sample. This affects not only the resonance frequencies of the individual modes, but also the strengths of the associated resonance peaks. Hence, the entire frequency spectrum of the transmission coefficient S_{21} varies with ε_r, and this has consequences for the UWB waveform as the UWB signal utilizes the frequency range from 3.1 to 5.3 GHz. The details are complicated because the cavity is highly overmoded at these frequencies, but the integral consequences are easily described according to Fig. 6: at high P_{Tx}, PER is zero regardless of ε_r as all packets are correctly received; at low P_{Tx}, PER is 100 % regardless of ε_r as all packets are corrupted by noise; and at intermediate power levels, PER depends on ε_r as different permittivities lead to different effective losses.

By attributing the known permittivities to each of the curves in Fig. 6, one obtains functions of the form PER(P_{Tx}, ε_r). At constant transmit power, this yields a characteristic curve of the form PER(ε_r; P_{Tx}). The result is shown in Fig. 7. It is obvious that ε_r can be estimated from PER unless ε_r becomes too large. The measurement range of this system would be from ε_r = 1 to about 10. The onset of the saturation is influenced by system details as the transmission power, the sample disc thickness, etc.

The sensitivity of the measurement system (slope of the curves in Fiq. 7) decreases with ε_r, but the rate at which it decreases depends on P_{Tx}. It is conceivable to use higher transmit powers for high-ε_r materials (the higher-P_{Tx} curves in Fiq. 7 are steeper at higher ε_r than the lower-P_{Tx} curves) and to use lower transmit powers for low-ε_r materials (the lower-P_{Tx} curves are steeper at low ε_r than the higher-P_{Tx} curves). But note that "high-ε_r" here means values on the order of 10, not 100 or 1000. If really high permittivities are to be measured, the sample disc must be placed near the ends of the cavity resonator (instead of at its center).

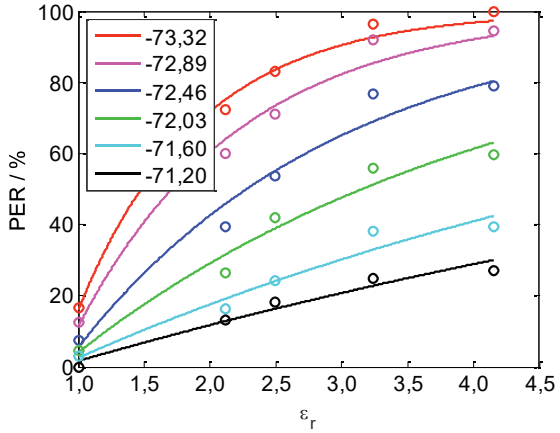

Fig. 7: Measured PER as a function of the sample permittivity with the transmit power as parameter (circles). The solid lines are fit curves of the form $\mathrm{PER}/\% = 100 - a \cdot \exp(-b \cdot \varepsilon_r)$ *with a, b according to Tab. 3.*

Tab. 3: Coefficients of the fit curves in Fig. 7.

Power P_{Tx} / dBm	*a*	*b*
–73.32	248.6	1.086
–72.89	197.8	0.804
–72.46	155.3	0.497
–72.03	129.9	0.303
–71.60	115.1	0.167
–71.20	109.6	0.108

The packet error ratio is a less than optimum measurand if one wants to design a fast measurement system. The packets on which Figs. 6 and 7 are based comprised 1023 four-byte words, or about 32 Kibit. As a data rate of about 75 kbit/s and a measurement time of 300 s were used, the measured PER was determined from the observation of roughly 700 packets. This should be enough to reliably measure the random variable PER to within a few percent. Although the characterization of materials does not require fast measurements, measurement times of 300 s are not readily accepted by users. At least, one would like to know the required minimum measurement time for a desired uncertainty in the measured PER.

To estimate the influence of the measurement time (in other words: of the number of packets sent and evaluated), we proceeded as follows:

1. Choose a cavity resonator with filling.
2. Fix the transmit power.
3. Fix the measurement time.
4. Measure the PER.
5. Repeat step 4 *N* times.
6. Compute the estimate for the expected value of PER and its uncertainty according to the *Guide to the Expression of Uncertainty in Measurement* (GUM) [12].

Fig. 8 shows the resulting complete measurement results for PER with an empty cavity resonator at a confidence level of 95 % (P_{Tx} = –73.83 dBm, N = 10). When an absolute PER uncertainty of, say, ±5 % is required, a measurement time of 30 s or so suffices. As the empty cavity is the worst case for the PER

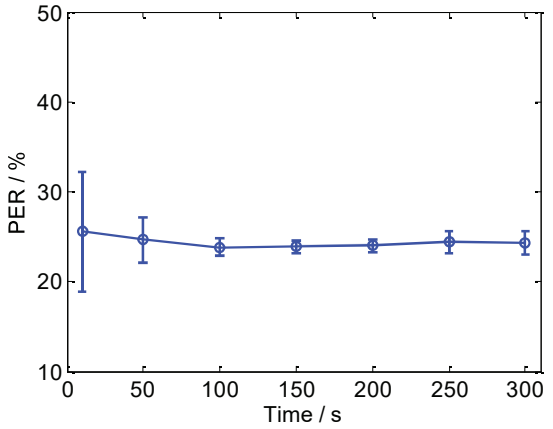

Fig. 8: Complete measurement result for PER with an empty cavity resonator as transmission channel as a function of the measurement time (confidence level of 95 %).

uncertainty (it is associated with the lowest PER values and therefore requires that more packets be observed to obtain a statistically valid estimate of PER), the characterization of material samples needs less time.

In addition to PER, we have also considered other stochastic system parameters which may allow a faster measurement. In the following, we discuss the autocorrelation functions of the time-domain receive-signal envelopes,

$$\Phi_{ii}(\tau) = \int_{-\infty}^{+\infty} e_i(t)\, e_i(t+\tau)\, \mathrm{d}t\,,$$

for different material discs. For each material, the waveform of the receive signal was measured five times at intervals of about 60 s. The five autocorrelation functions computed from these measurements were normalized to 1, averaged and then normalized to the maximum value of the first autocorrelation function (to convey some idea of the actual magnitude of the function). The results for $P_{Tx} = -64.62$ dBm are shown in Fig. 9.

An increase in ε_r clearly leads to higher signal attenuation or a lower receive-signal power, which is proportional to $\Phi_{ii}(0)$. This is explained as follows: with a higher-permittivity material in the cavity center, the electric field concentrates in this region and less so around the feeds. As a consequence, less power is coupled into and out of the cavity. Hence, less power is received by the communication sink.

The value of ε_r also exerts some influence on the width of $\Phi_{ii}(\tau)$: the curves become the narrower, the higher ε_r. Last but not least, the sequence of the curves in Fig. 9 is the same as observed with VNA measurements.

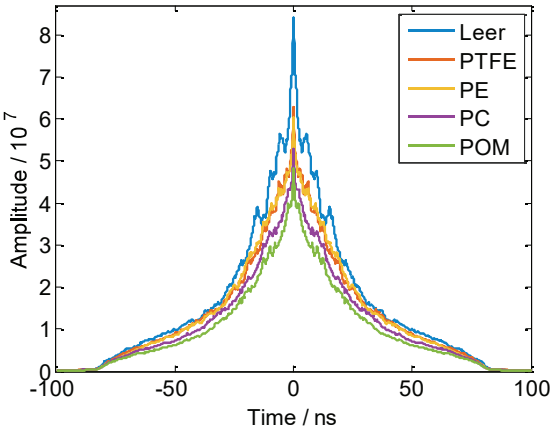

Fig.9: Autocorrelation functions of measured receive-signal envelopes for different materials in the communication channel (= cavity resonator).

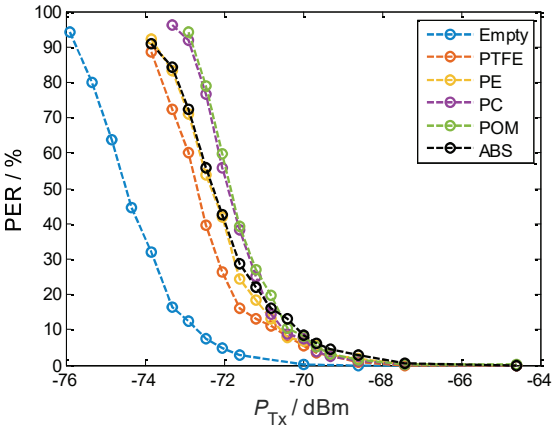

Fig. 10: Fig. 6 repeated and supplemented with the curve produced with an ABS sample.

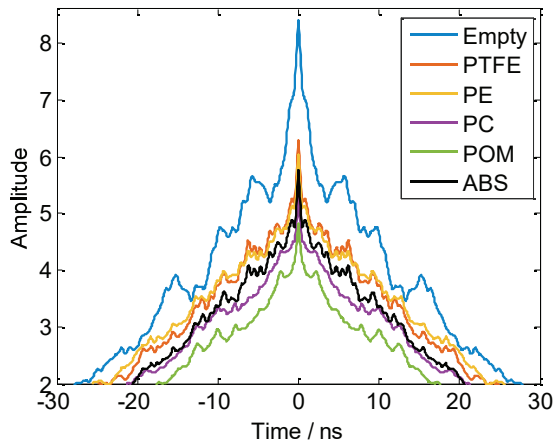

Fig. 11: Fig. 9 repeated (and zoomed) and supplemented with the curve produced using ABS.

Figs. 10 and 11 respectively show the measured curves of Figs. 6 and 9, but supplemented with the curve obtained for the ABS sample. From these data, one can classi-

Tab. 4: Dielectric constant of the ABS sample measured at different transmit powers (based on the fit curves from Fig. 7).

P_{Tx} / dBm	PER / %	ε_r
–73.32	84.39	2.55
–72.89	72.45	2.45
–72.46	55.93	2.54
–72.03	42.52	2.69

fy the ABS permittivity as lying between that of PE (2.43) and that of PC (3.06). The quantitative results are listed in Table 4, where we have restricted ourselves to comparatively smaller transmit powers to meet the requirements discussed above (smaller transmit powers for smaller-ε_r materials). The numerical values are consistent with the range known from the literature (Table 1).

Conclusions

We have presented a measurement system based on the statistics of a radio communication system, which allows one to measure the dielectric permittivity of samples inside a microwave cavity resonator.

It was demonstrated experimentally by way of various material compositions, that the radio channel characteristics are affected strongly enough to allow the measurement of the dielectric constant from the stochastic signal parameters. The results show a good agreement with those achieved by a more standard LCR meter.

We believe that the architecture of our novel system can be implemented at low cost in the field. This would further the goal of cost-efficient in-situ diagnostics. However, depending on the dynamic requirements of the application, one must carefully choose the random variables to be measured. We have shown that working with the "wrong" variable – such as the packet error rate determined from the transmission of very long packets – can lead to inordinately long measurement times (on the order of tens of seconds).

References

[1] J. M. Catala-Civera et al., "Dynamic Measurement of Dielectric Properties of Materials at High Temperature During Microwave Heating in a Dual Mode Cylindrical Cavity," *IEEE Trans. MTT*, vol. 63, no. 9, pp. 2905–2914, Sept. 2015, doi: 10.1109/TMTT.2015.2453263.

[2] T. C. Baum, K. Ghorbani, "Measurements on the Effects of Moisture on the Complex Permittivity of High Temperature Ash," *IEEE Trans. MTT*, vol. 64, no. 2, pp. 607–615, Feb. 2016. doi: 10.1109/TMTT.2015.2512595.

[3] A. Sappok, L. Bromberg, "Radio Frequency Diesel Particulate Filter Soot and Ash Level Sensors: Enabling Adaptive Controls for Heavy-Duty Diesel Applications," *SAE Int'l J. Comm. Vehicles*, 7 (2014) 468-47, doi: 10.4271/2014-01-2349.

[4] I. Motroniuk, R. Królak, R. Stöber, G. Fischerauer, "State Observation in Automotive Aftertreatment Systems Based on Wireless Communication Links," *Proc. 5th IMEKO TC19 Symp. Environmental Instrumentation and Measurements*, Chemnitz, pp. 122–126, Sept. 23–24, 2014.

[5] I. Motroniuk, R. Stöber, G. Fischerauer, "State determination of catalytic converters based on an ultra-wideband communication system," *J. Sens. Sens. Syst.*, vol. 4, pp. 255–262, Aug. 2015, doi: 10.5194/jsss-4-255-2015.

[6] K. D. Wong, *Fundamentals of wireless communication engineering technologies*. Hoboken, NJ: John Wiley & Sons, pp. 481–485, 2012.

[7] Product data sheet, "PulsON P410," Time Domain, Nov. 2013.

[8] H. Marko, *Methoden der Systemtheorie* (in German). Berlin etc.: Springer, 114 ff. (^{2}1982).

[9] G. Menges, E. Haberstroh, W. Michaeli, E. Schmachtenberg, *Werkstoffkunde Kunststoffe* (in German). München: Hanser, 6th ed. 2011, p. 316.

[10] Product data sheets, "Werkstoff-Datenblätter : Technische Kunststoffe und deren Eigenschaften," Kern GmbH, <www.kern-gmbh.de/index.html?/kunststoff/service/werkstoffe/eigenschaften/datenblatt.htm>, (2014).

[11] J. Baker-Jarvis, M. Janezic, D. DeGroot, „High-Frequency Dielectric Measurements," *IEEE IM Magazine*, Vol. 13, Issue 2, pp. 24–31, Apr. 2010.

[12] ISO/IEC Guide 98-3:2008, „Uncertainty of measurement — Part 3: Guide to the expression of uncertainty in measurement".